Photocatalytic Water Splitting with the Cr-Doped $Ba_2In_2O_5/In_2O_3$ Composite Oxide Semiconductors

Defa Wang,[†,‡] Zhigang Zou,[§] and Jinhua Ye*[,†,‡]

Ecomaterials Center, National Institute for Materials Science (NIMS), 1-2-1 Sengen, Tsukuba, Ibaraki 305-0047, Japan, Precursory Research for Embryonic Science and Technology (PREST), Japan Science and Technology Agency (JST), 4-1-8 Hon-cho Kawaguchi-shi, Saitama 332-0012, Japan, and Ecomaterials and Renewable Energy Research Center (ERERC), Nanjing University, 22 Hankou Road, Nanjing 210093, China

Received December 30, 2004. Revised Manuscript Received April 18, 2005

The Cr-doped $Ba_2In_2O_5/In_2O_3$ (C−BIO) oxide semiconductors synthesized by a solid-state reaction method were found to be a novel composite photocatalyst system with enhanced activity for water splitting. The C−BIO powder samples were characterized with X-ray diffraction (XRD), UV−vis diffuse reflectance spectrometry, energy dispersive spectrometry (EDS), and high-resolution transmission electron microscopy (HRTEM). The photocatalytic activities of Pt- or NiO-loaded C−BIO and individual precursor materials were evaluated by H_2 evolution from aqueous CH_3OH solution under visible light and by pure water splitting under UV light irradiation, respectively. It was found that the composite C−BIO showed a higher H_2 evolution rate in comparison with individual materials. The overall band structure, charge carrier excitation, separation, and transportation and the redox reactions for H_2 and O_2 evolution in the C−BIO system are discussed in relation to the photophysical and photocatalytic properties, and some guidelines are suggested for designing efficient composite semiconductor photocatalysts for water splitting.

1. Introduction

In view of global energy and environmental issues, photocatalytic water splitting to produce clean energy H_2 has been widely regarded as one of the ideal solar energy conversion methods.[1,2] Generally, the process of photocatalytic water splitting with a semiconductor includes several reactions: (1) photoinduced intrinsic ionization of a semiconductor over the band gap, resulting in the formation of electrons in the conduction band and holes in the valence band: $2h\nu \rightarrow 2e + 2h$; (2) oxidization of water by holes: $2h + H_2O \rightarrow 1/2O_2 + 2H^+$ at the valence band; and (3) reduction of hydrogen ions by electrons: $2H^+ + 2e \rightarrow H_2$ at the conduction band. In principle, the previously mentioned reactions can be realized either by a one-photon excitation process or by a two-photon excitation process (Z-scheme).[3] In both cases, the most crucial prerequisite to photocatalytic water splitting is that the band edges of a photocatalyst must be suitable for the redox reactions of H_2 and O_2 evolution.

Much effort has been made to develop single-phased photocatalysts for efficient water splitting. To our knowledge, however, the number of single-phased photocatalysts capable of stoichiometric water splitting, especially under visible light irradiation, is still very limited so far.[2−13] In fact, modulation of the electronic structure of a semiconductor is restricted to some extent within a given crystal structure. On the other hand, we consider two semiconductors, neither of which is able to realize stoichiometric water splitting probably because of the rapid recombination of photoexcited electron/hole pairs,[2] even though their band edges are suitable for both H_2 and O_2 evolution. In principle, if these two semiconductors are integrated into one system, this system will be able to fulfill the redox reactions of both H_2 and O_2 evolution and thus can be expected theoretically to be a photocatalytic system for stoichiometric water splitting. Actually, designing composite semiconductor photocatalysts to achieve efficient charge separations in a light energy conversion system has attracted much attention.[14−21] One of the successful examples,

* Corresponding author. Fax: +81-298-59-2601; e-mail: jinhua.ye@nims.go.jp.
† National Institute for Materials Science.
‡ Japan Science and Technology Agency.
§ Nanjing University.

(1) Fujishima, A.; Honda, K. *Nature* **1972**, *238*, 37.
(2) Linsebigler, A. L.; Lu, G. Q.; Yates, J. T. *Chem. Rev.* **1995**, *95*, 735.
(3) Kudo, A. *J. Ceram. Soc. Jpn.* **2001**, *109*, S81.
(4) Zou, Z.; Ye, J.; Sayama, K.; Arakawa, H. *Nature* **2001**, *414*, 6254.
(5) Domen, K.; Kondo, J. N.; Hara, M.; Takata, T. *Bull. Chem. Soc. Jpn.* **2000**, *73*, 1307.
(6) Zou, Z.; Ye, J.; Sayama, K.; Arakawa, H. *J. Photochem. Photobiol., A* **2002**, *148*, 65.
(7) Kudo, A.; Mikami, I. *Chem. Lett.* **1998**, 1027.
(8) Sato, J.; Saito, S.; Nishiyama, H.; Inoue, Y. *J. Phys. Chem.* **2001**, *105*, 6061.
(9) Sato, J.; Saito, N.; Nishiyama, H.; Inoue, Y. *Chem. Lett.* **2001**, 868.
(10) Yin, J.; Zou, Z.; Ye, J. *J. Mater. Res.* **2002**, *17*, 2201.
(11) Sato, J.; Saito, S.; Nishiyama, H.; Inoue, Y. *J. Phys. Chem.* **2003**, *107*, 7975.
(12) Hara, M.; Nunoshige, J.; Takata, T.; Kondo, J. N.; Domen, K. *Chem. Commun.* **2003**, 3000.
(13) Ishikawa, A.; Yamada, Y.; Takata, T.; Kondo, J. N.; Hara, M.; Kobayashi, H.; Domen, K. *Chem. Mater.* **2003**, *15*, 4442.
(14) Kraeutler, B.; Bard, A. J. *J. Am. Chem. Soc.* **1978**, *100*, 4317.
(15) Spanhel, L.; Weller, H.; Henglein, A. *J. Am. Chem. Soc.* **1987**, *109*, 6632.
(16) Gopidas, K. R.; Bohorquez, M.; Kamat, P. V. *J. Phys. Chem.* **1990**, *94*, 6435.
(17) Lawless, D.; Kapoor, S.; Meisel, D. *J. Phys. Chem.* **1995**, *99*, 10329.
(18) Vogel, R.; Hoyer, P.; Weller, H. *J. Phys. Chem.* **1994**, *94*, 3183.
(19) Evans, J. E.; Springer, K. W.; Zhang, J. Z. *J. Chem. Phys.* **1994**, *101*, 6222.
(20) Sant, P. A.; Kamat, P. V. *Phys. Chem. Chem. Phys.* **2002**, *4*, 198.

10.1021/cm0477117 CCC: $30.25
Published on Web 05/18/2005

except for the fatal photoanodic corrosion of CdS, is the well-known CdS/TiO_2 composite semiconductor system, of which the photocatalytic activity for reduction of methyl viologen was drastically increased under visible light irradiation.[15] Recently, Sayama and Abe et al. reported another example that stoichiometric splitting of water under visible light irradiation was realized over a mixture of $Pt-WO_3$ and $Pt-SrTiO_3$ (codoped with Cr/Ta) photocatalysts and the IO_3^-/I^- shuttle redox mediator.[22−25]

However, in the previously mentioned composite semiconductor systems, in which the two semiconductors are simply coupled or mediated with a shuttle redox, the charge transportation between two semiconductors seems to not be fluent although the charge separation ability is improved. On the contrary, if the individual semiconductors are well-alloyed to form an ohmic contact, both the charge transportation ability and the charge separation ability shall be promoted significantly, leading to an improved photocatalytic activity consequently. Up to now, various kinds of indates such as $In_2O_3(ZnO)_m$,[7] MIn_2O_4 (M = Ca, Sr, Ba),[8−10] $LnInO_3$ (Ln = La, Nd), and $Sr_{1-x}M_xIn_2O_4$ (M = Ca, Ba)[11] have been reported as photocatalysts for water splitting. However, the activities of the aforementioned In^{3+}-containing photocatalysts are usually low under visible light irradiation due to the relatively large band gaps. On the other hand, the Cr 3d orbitals have been paid much attention in developing visible-light-driven photocatalysts. For example, new absorption peaks in the visible light region have been observed in Cr-doped and Cr/Sb-codoped TiO_2[26−31] and $SrTiO_3$,[32] which show activity for H_2 evolution. Our previous study also showed that the split Cr 3d orbitals in the spinel type photocatalyst $BaCr_2O_4$ played a key role in H_2 evolution under visible light irradiation.[33] Recently, we have succeeded in the development of a composite photocatalyst, the Zn-doped Lu_2O_3/Ga_2O_3 (Z-LGO), for stoichiometric water splitting under UV light irradiation.[34] In present paper, we report the Cr-doped $Ba_2In_2O_5/In_2O_3$ (C−BIO) oxide semiconductors as a novel composite photocatalysis system for water splitting, in which the afore-mentioned points such as the charge separation and transportation as well as the effect of Cr doping have been incorporated into the design strategy. The phase constituents, microstructures, photophysical properties, and photocatalytic activities of the C−BIO system are systematically investigated. Some strategies for designing efficient composite photocatalysts for water splitting are proposed.

2. Experimental Procedures

2.1. Photocatalyst Preparation. The C−BIO powder samples were synthesized by conventional solid-state reaction methods. First, Cr-doped $Ba_2In_2O_5-Ba_2(In_{0.95}Cr_{0.05})_2O_5$ ($Cr-Ba_2In_2O_5$) and Cr-doped $In_2O_3-(In_{0.95}Cr_{0.05})_2O_3$ ($Cr-In_2O_3$) were presynthesized by heating a mixture of $BaCO_3 + In_2O_3 + Cr_2O_3$ (Wako, purity: 99.9%) in a molar ratio of 2:0.95:0.05 and a mixture of $In_2O_3 + Cr_2O_3$ (Wako, purity: 99.9%) in a molar ratio of 0.95:0.05 at 900 °C for 12 h and then at 1100 °C for 24 h, respectively. Next, a mixture of presynthesized $Cr-Ba_2In_2O_5$ and $Cr-In_2O_3$ in a molar ratio of 1:1 were calcined at 1100 °C for 24 h in an alumina crucible in air, forming the C−BIO powder samples.

For photocatalytic H_2 evolution from aqueous CH_3OH solution as a sacrificial reagent, the cocatalyst Pt (0.5 wt %) was loaded on the surface of C−BIO powder samples by an in situ photodeposition method:[6] under light irradiation, an equivalent molar amount of H_2PtCl_6 in solution was reduced to the metallic state and deposited onto the surface of catalyst, forming the photocatalyst Pt (0.5 wt %)/C−BIO. For photocatalytic splitting of pure water, the cocatalyst NiO_x (1.0 wt %) was loaded on the surface of the C−BIO powder samples using an impregnation method:[6] the powder samples were sunk into equivalent molar amounts of an aqueous $Ni(NO_3)_2 \cdot 6H_2O$ solution and calcined at 500 °C for 2 h, forming the photocatalyst NiO_x (1.0 wt %)/C−BIO.

2.2. Photocatalyst Characterization. The synthesized C−BIO powder samples were examined by X-ray diffraction (XRD, JEOL JDX-3500) using CuKα radiation (λ = 1.54178 Å). A scanning electron microscope (SEM, JEOL JSM-5400) and a high-resolution transmission electron microscope (HRTEM, JEOL JEM-2010, operated at 200 kV), both of which were equipped with an energy dispersive spectrometer (EDS), were employed for microstructure characterization and composition analysis. A UV−vis diffuse reflectance spectrum was measured with a UV−vis spectrometer (Shimadzu UV-2500) and was converted from reflection to absorption spectrum by the Kubelka−Munk method.

2.3. Photocatalytic Activities. Photocatalytic reactions were carried out in a closed gas circulation system, to which the reaction cells containing the respective solutions were connected. Before reaction, the closed gas circulation system and reaction cells were well-evacuated and then introduced to ~2.5 kPa argon gas. The reaction under visible light irradiation ($\lambda \geq 420$ nm) was performed in a Pyrex glass cell (270 mL) with a side window, to which the light from a 300 W xenon arc lamp (ILC Technology, CERMAX LX-300, operated at 200 W) was irradiated through a long-pass cutoff filter (HOYA, L42). For photocatalytic H_2 evolution from an aqueous CH_3OH solution dispersed with Pt (0.5 wt %)/C−BIO powders (0.5 g), the sacrificial reagent methanol (50 mL) was taken as an electron donor. For photocatalytic O_2 evolution from aqueous $AgNO_3$ solution (H_2O 370 mL, $AgNO_3$ 5 mmol) dispersed with C−BIO powders (0.5 g), the sacrificial reagent silver nitrate ($AgNO_3$) was taken as an electron acceptor. Photocatalytic splitting of pure water under UV light irradiation was carried out by dispersing the NiO_x (1.0 wt %)/C−BIO powder photocatalyst (0.5 g) in an inner irradiation quartz cell (370 mL). The light source was a 400 W high-pressure mercury lamp (RIKO 400HA). With an increase of irradiation time, gases were evolved, and the the gas pressure was increased. The gases were in situ analyzed with a TCD gas chromatograph (Shimadzu GC-8AIT, argon carrier), which was connected to the closed gas circulating line. The apparent

(21) Liu, D.; Kamat, P. V. *J. Phys. Chem.* **1993**, *97*, 10769.
(22) Sayama, K.; Makasa, K.; Abe, R.; Abe, Y.; Arakawa, H. *Chem. Commun.* **2001**, 2416.
(23) Abe, R.; Sayama, K.; Domen, K.; Arakawa, H. *Chem. Phys. Lett.* **2001**, *344*, 339.
(24) Abe, R.; Sayama, K.; Arakawa, H. *Chem. Phys. Lett.* **2003**, *379*, 230.
(25) Abe, R.; Sayama, K.; Arakawa, H. *Chem. Phys. Lett.* **2003**, *371*, 360.
(26) Yamashita, H.; Ichihashi, Y.; Takeuchi, M.; Kishiguchi, S.; Anpo, M. *J. Synchrotron Radiat.* **1999**, *6*, 451.
(27) Choi, W.; Termin, A.; Hoffmann, M. R. *J. Phys. Chem.* **1994**, *98*, 13669.
(28) Palmisano, L.; Augugliaro, V.; Sclafani, A.; Schiavello, M. *J. Phys. Chem.* **1988**, *92*, 6710.
(29) Matsumoto, Y.; Kurimoto, J.; Shimizu, T.; Sato, E. *J. Electrochem. Soc.* **1981**, *128*, 1040.
(30) Fuerte, A.; Hernandez-Alonso, M. D.; Maira, A. J.; Martinez-Arias, A.; Fernandez-Garcia, M.; Conesa, J. C.; Soria, J. *Chem. Commun.* **2001**, 2718.
(31) Umebayashi, T.; Yamaki, T.; Itoh, H.; Asai, K. *J. Phys. Chem. Solids* **2002**, *63*, 1909.
(32) Kato, H.; Kudo, A. *J. Phys. Chem. B* **2002**, *106*, 5029.
(33) Wang, D. F.; Zou, Z. G.; Ye, J. H. *Chem. Phys. Lett.* **2003**, *373*, 191.

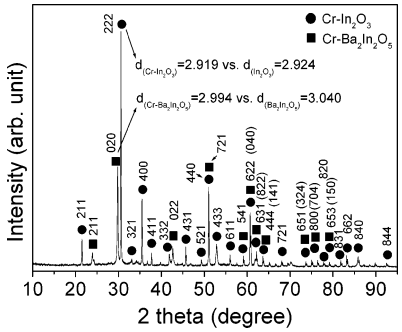

Figure 1. X-ray diffraction pattern of the C−BIO powder sample at room temperature. The indexed result shows that C−BIO is mainly comprised of Cr−In_2O_3 and Cr−$Ba_2In_2O_5$. Compared with the diffraction patterns of In_2O_3 and $Ba_2In_2O_5$, the peak positions of Cr−In_2O_3 and Cr−$Ba_2In_2O_5$ shift toward a larger 2θ, and the d values of Cr−In_2O_3 and Cr−$Ba_2In_2O_5$ decrease as shown, for example, by two representative atomic planes.

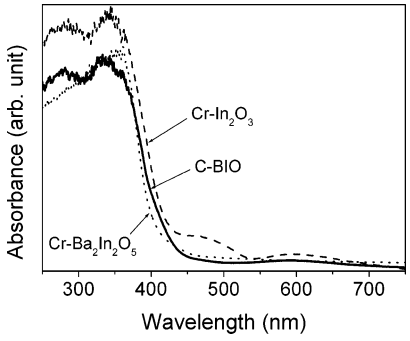

Figure 2. UV−vis diffuse reflectance spectra of C−BIO and individual Cr-doped raw materials at room temperature.

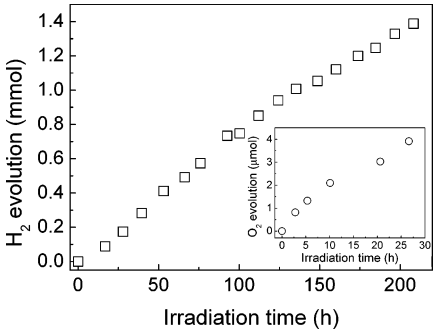

Figure 3. H_2 evolution from aqueous CH_3OH solution dispersed with Pt (0.5 wt %)/C−BIO (0.5 g, 1.2 mmol) and (inset) O_2 evolution from an aqueous $AgNO_3$ solution dispersed with C−BIO (0.5 g, 1.2 mmol) under visible light irradiation. Light source: 300 W Xe lamp, cutoff filter ($\lambda > 420$ nm).

quantum yield (Q.Y.)—the ratio of the number of reacted electrons to the number of incident photons—was measured using interference band-pass filters (MIF-W, Kenko).

3. Results and Discussion

3.1. Materials Characterization. (A) Crystal Structures and Phase Constitutions in C−BIO. Figure 1 shows the XRD pattern and indexed result of the synthesized C−BIO powder sample at room temperature. We can see that, except for very few weak peaks of impurities, almost all the peaks could be assigned as Cr−In_2O_3 and Cr−$Ba_2In_2O_5$. The few unknown impurities are probably an alloy (or solid solution) created at the interface between Cr−In_2O_3 and Cr−$Ba_2In_2O_5$ during the annealing treatment. This alloy, as will be discussed in the section 3.3, is expected to play an important role in tailoring the electronic property of Cr−In_2O_3 and Cr−$Ba_2In_2O_5$. As compared with the diffraction patterns of In_2O_3 and $Ba_2In_2O_5$,[35,36] the peaks of Cr−In_2O_3 and Cr−$Ba_2In_2O_5$ shifted toward a larger 2θ, indicating the decrease of lattice parameters because the effective ionic radius of Cr^{3+} (0.615 Å) is smaller than that of In^{3+} (0.800 Å).[37] The EDS analysis results confirmed that the overall composition was consistent with those of the as-designed C−BIO, and the doped Cr was distributed homogeneously. It is assumed that the substitution of Cr^{3+} for In^{3+} in both Cr−$Ba_2In_2O_5$ and Cr−In_2O_3 has kept the charge balance in the C−BIO system. Before and after photocatalytic reactions, the color of samples was grayish green—the typical color of Cr^{3+} doped oxides.[38] It implied that the valence state of Cr ions doped in C−BIO did not change during photocatalytic reactions.

(B) UV−vis Diffuse Reflectance Spectra. UV−vis diffuse reflectance spectra of C−BIO and Cr-doped individual materials are shown in Figure 2. Although it is not a single-phased compound, C−BIO shows a main absorption edge around 440 nm, which seems to be the linear combination of Cr-doped individual materials (∼430 nm for Cr−$Ba_2In_2O_5$ and ∼450 nm for Cr−In_2O_3). In comparison with the raw materials $Ba_2In_2O_5$ and In_2O_3, the band gap energies of Cr−$Ba_2In_2O_5$ and Cr−In_2O_3 did not decrease so much, indicating that the doped Cr 3d orbitals seemed to form discrete shallow bands within the forbidden bands of $Ba_2In_2O_5$ and In_2O_3, as in the cases of Fe-doped TiO_2.[39,40] The absorption peak between 550 and 650 nm could be ascribed to the doped Cr 3d orbitals. The well-hybridized absorption edge of C−BIO implied that both band gaps and band edges of individual materials in C−BIO were compatible with each other very well. Considering the fact that the calcining temperature and duration time were sufficient for the process of atomic alloying, we speculated that an ohmic contact was likely to form among the components of C−BIO, thus enabling fluent interparticle charge transportation. This can be considered as one of important factors for the enhanced activity of a composite semiconductor system in terms of interfacial charge-transfer kinetics.

3.2. Photocatalytic Activities. (A) H_2 Evolution in the Presence of CH_3OH as Sacrificial Reagent. Figure 3 shows photocatalytic H_2 evolution from aqueous methanol solution (50 mL of CH_3OH + 220 mL of H_2O) with a powder suspension of Pt (0.5 wt %)/C−BIO (0.5 g) photocatalyst under visible light irradiation ($\lambda \geq 420$ nm). We can see that considerable amount of H_2 was evolved upon light irradiation. A dark test showed that almost no H_2 was evolved when the light was turned off. The apparent quantum yield (Q.Y.) at $\lambda = 420.4$ nm was measured to be only ∼0.3% by

(34) Wang, D. F.; Zou, Z. G.; Ye, J. H. *Chem. Phys. Lett.* **2004**, *384*, 139.
(35) Fischer, W.; Reck, G.; Schober, T. *Mater. Sci. Forum* **2000**, *321*, 363.
(36) Nadaud, N.; Lequeux, N.; Nanot, M.; Jove, J.; Roisnel, T. *J. Solid State Chem.* **1998**, *135*, 140.
(37) Shannon, R. D. *Acta Crystallogr.* **1976**, *A32*, 751.
(38) Pavlov, R. S.; Marza, V. B.; Carda, J. B. *J. Mater. Chem.* **2002**, *12*, 2825.
(39) Wang, C.-y; Bahnemann, D. W.; Dohrmann, J. K. *Chem. Commun.* **2000**, 1539.
(40) Wang, C.-y; Bottcher, C.; Bahnemann, D. W.; Dohrmann, J. K. *J. Mater. Chem.* **2003**, *13*, 2322.

Table 1. Photocatalytic Evolution Rates (μmol/h) of H_2 and O_2 with C−BIO and Individual Materials

	visible light		UV light	
	Pt/catalyst + CH_3OH solution	catalyst + $AgNO_3$ solution	NiO/catalyst + pure water	
photocatalysts	H_2	O_2	H_2	O_2
C−BIO[a]	7.9	0.35	29.3	15.2
BIO[b]	1.2	0.2	7.8	0
In_2O_3	0.36	1.30	1.1	0
$Cr-In_2O_3$	0.3	0.35	0.7	0
$Ba_2In_2O_5$	3.2	0.46	4.2	0
$Cr-Ba_2In_2O_5$	1.1	0	1.3	0

[a] C−BIO: Cr-doped $Ba_2In_2O_5/In_2O_3$, calcined at 1100 °C for 24 h. [b] BIO: $Ba_2In_2O_5/In_2O_3$ calcined at 1100 °C for 24 h.

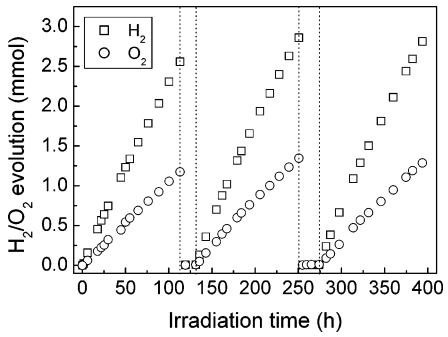

Figure 4. Long time course of stoichiometric water splitting over NiO_x (1.0 wt %)/C−BIO (0.5 g, 1.2 mmol) under UV light irradiation. Light source: 400 W high-pressure Hg lamp (RIKO-400A).

using an interference band-pass filter ($\lambda_0 = 420.4$ nm, $T_{max} = 44.8\%$, $\Delta\lambda/2 = 14.7$ nm). Nevertheless, the synthesized C−BIO was confirmed to hold the potential for photocatalytic H_2 evolution under visible light irradiation.

(B) O_2 Evolution in the Presence of $AgNO_3$ as Sacrificial Reagent. Photocatalytic O_2 evolution from an aqueous $AgNO_3$ solution (270 mL of H_2O + 5 mmol of $AgNO_3$) with a powder suspension of C−BIO photocatalyst (0.5 g) was carried out, and the result is also shown in Figure 3 (inset). Although the evolution rate of O_2 was lower than that of H_2, the generation of O_2 indicated that the synthesized C−BIO also held the potential for O_2 evolution under visible light irradiation.

(C) Stoichiometric Splitting of Pure Water. The aforementioned results suggested that the composite C−BIO possessed the potentials for photocatalytic evolution of both H_2 and O_2, implying the possibility of overall water splitting over C−BIO. An attempt to decompose pure water with a NiO_x (1.0 wt %)/C−BIO (0.5 g) powder sample did not succeed under visible light irradiation probably due to the too low photocatalytic activity in the absence of sacrificial reagents. Fortunately, stoichiometric water splitting was realized over a NiO_x (1.0 wt %)/C−BIO (0.5 g) powder sample under UV light irradiation, and the result is shown in Figure 4. The amount of evolved H_2/O_2 gases increased linearly with an increase of irradiation time, while no gases were evolved upon turning off the light. No sign of deactivation was observed even after a long term of reaction for about 350 h, indicating that the as-prepared sample was stable under UV light irradiation. The average evolution rates were about 29.3 μmol/h for H_2 and 15.2 μmol/h for O_2, respectively. The apparent quantum yield (Q.Y.) at $\lambda = 320$ nm was measured to be ~4.2% by using an interference band-pass filter ($\lambda_0 = 320$ nm, $T_{max} = 20.1\%$, $\Delta\lambda/2 = 15.7$ nm). The accumulative molar amount of gases evolved during each reaction cycle of ~115 h was twice more than the molar amount of C−BIO catalysts used. The turnover number—the ratio of the total amount of gas evolved to the catalyst used (1.2 mmol in this system)—exceeded 7 after reacting for 350 h. In terms of reacted electrons relative to the NiO_x loaded on the catalyst surface, the turnover number reached 123 after reacting for 350 h. These results confirmed that the gas evolution had been a catalytic process intrinsically.

It should be pointed out that the aforementioned photocatalytic reactions were also carried out under the same conditions for individual materials and, particularly, for the composite $Ba_2In_2O_5/In_2O_3$ (BIO) without Cr doping, which were synthesized by calcining In_2O_3 and presynthesized $Ba_2In_2O_5$ at 1100 °C for 24 h. Table 1 summarizes the photocatalytic activities of the composite systems C−BIO, BIO, and individual materials with and without Cr doping. It clearly shows that, in the presence of CH_3OH as a sacrificial reagent, the H_2 evolution rate of C−BIO was much higher than those of BIO and individual materials with or without Cr doping. No individual materials, with or without Cr doping, were able to split pure water stoichiometrically. Only H_2 was evolved but at much lower rates as compared with that of C−BIO. $Ba_2In_2O_5$ has been found to suffer instability in water.[10,41] As a component in the composite C−BIO system, $Cr-Ba_2In_2O_5$ was not observed unstable in water even under UV and visible light irradiation. We also noticed that the evolution rates of H_2 or O_2 over both $Cr-Ba_2In_2O_5$ and $Cr-In_2O_3$ in the presence of respective sacrificial reagents were increased or decreased, more or less, in comparison with the raw materials without Cr doping. It indicated that the evolution rates of H_2 and O_2 were influenced by Cr doping. In general, the composite C−BIO had great advantages over the individual materials for photocatalytic water splitting.

3.3. HRTEM Observations on the Composite Nanostructures of C−BIO. The functional properties of composite nanomaterials can be greatly improved by coupling the semiconductor or metal nanocluster with another type of compatible materials.[42] Semiconductor−metal nanocomposite particles have been found useful to improve the efficiency of photocatalytic and photoelectrochemical conversion of light energy because of improvement of the interfacial charge-transfer kinetics. Platinized TiO_2 (Pt/TiO_2),

(41) Hashimoto, T.; Inagaki, Y.; Kiski, A.; Dokiya, M. *Solid State Ionics* **2000**, *128*, 227.
(42) Adams, D. M.; Brus, L.; Chidsey C. E. D. et al. *J. Phys. Chem. B* **2003**, *107*, 6668.

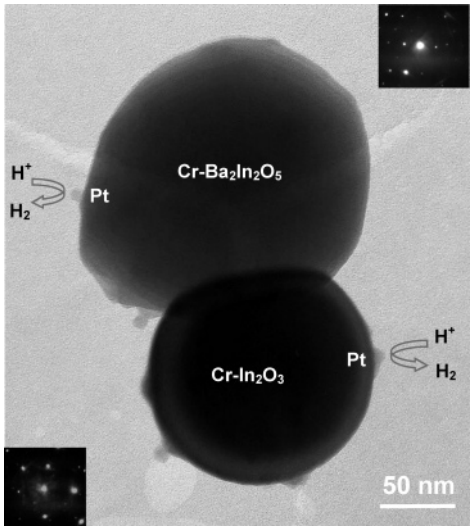

Figure 5. Typical TEM micrograph and SAED patterns taken from different particles of the composite C−BIO loaded with Pt nanoparticles. The indexed result showed that the C−BIO was composed of $Cr-Ba_2In_2O_5$ and $Cr-In_2O_3$, which were well-alloyed so that an ohmic contact was likely to form between each other. The Pt nanoparticles photodeposited on the C−BIO surface were supposed to be active sites for H_2 evolution due to the significant reduction of overpotential for H_2 evolution. Electron beam//$[0, 0, -1]_{Ba2In2O5}$//$[0, 1, -1]_{In2O3}$.

for instance, has been frequently used in photoreactions for the purpose of enhancing the reaction rates of water splitting,[43,44] hydrogen evolution from an alcohol−water solution,[45,46] and oxidization of organic compounds.[47−49] Noble metals such as Pt in a semiconductor photocatalysis system can change the photocatalytic process by changing the semiconductor surface properties. Usually, the yield of a particular product or the rate of the photocatalytic reaction can be enhanced by the addition of noble metals. The nanosized Pt particles loaded on the photocatalyst surface are supposed to be the active sites for H_2 evolution because of the trapping of electrons at the metal sites.[2] In the present composite C−BIO system, Pt was in situ photodeposited onto the surface of C−BIO for H_2 evolution by taking CH_3OH as a sacrificial reagent, and NiO was loaded onto the surface of C−BIO by an impregnation method for splitting pure water.

Extensive HRTEM observations and selected area electron diffraction (SAED) showed that the composite C−BIO powder sample was actually composed of $Cr-Ba_2In_2O_5$ and $Cr-In_2O_3$ as the XRD analysis confirmed. In most areas, the particle sizes of $Cr-Ba_2In_2O_5$ and $Cr-In_2O_3$ were quite different ranging from several tens to several hundreds of nanometers probably due to different sizes of individual raw materials. Figure 5 shows a typical HRTEM micrograph of the composite Pt/C−BIO consisting of two particles, on the surface of which the Pt nanoparticles were photodeposited.

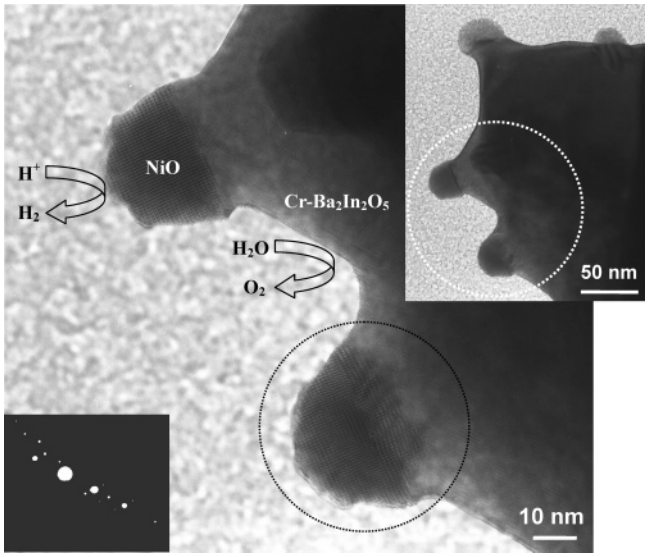

Figure 6. HRTEM micrograph and SAED pattern taken from the circled area of NiO_x/C−BIO after the reaction for pure water splitting under UV light irradiation. The indexed result showed that the NiO nanoparticles were capped mainly on $Cr-Ba_2In_2O_5$ in this area. The nanosized cocatalyst NiO_x is supposed to be the active site for H_2 evolution.

The indexed results of SAED patterns (inset) taken from different particles showed that these two particles were coincidently $Cr-Ba_2In_2O_5$ and $Cr-In_2O_3$, respectively. Although the electrical conductivity of C−BIO was not measured, we could see from Figure 5 that the two different particles were alloyed so well after calcining at 1100 °C for 24 h that an ohmic contact might be expected to form between these two particles. HRTEM images observed in other areas also confirmed the well contact condition among particles belonging to different phases or having different crystal orientations, even in atomic scales (see Supporting Information). As in the case of Pt loaded TiO_2 observed by Pichat et al.,[50] the photodeposited Pt nanoparticles with a mean size of ∼10 nm could be clearly observed on the surfaces of both $Cr-Ba_2In_2O_5$ and $Cr-In_2O_3$. These nanosized Pt particles were supposed to be active reaction sites due to the significant reduction of overpotential for H_2 evolution.

The nanoparticles of cocatalyst NiO[51,52] or RuO_2[53] on the surface of a photocatalyst usually act as a trapping center for either holes or electrons depending on the types of photocatalysts and reactions. Figure 6 shows the HRTEM micrograph and SAED patterns (inset) of the nanocomposite NiO_x/C−BIO after reaction for pure water splitting under UV light irradiation. In the NiO_x/C−BIO system, NiO_x was calcined onto the surface of C−BIO using an impregnation method. The matrix catalyst loaded with NiO_x was indexed to be $Cr-Ba_2In_2O_5$. In this case, the NiO_x particles of ∼20 nm behaved, similarly to the case of $NiO_x/SrTiO_3$,[51] as the active sites for H_2 evolution. In general, the presence of nanosized cocatalysts Pt and NiO significantly reduces the overpotentials for H_2 and O_2 evolution, respectively.[2,51]

(43) Sato, S.; White, J. M. *Chem. Phys. Lett.* **1980**, *72*, 83.
(44) Sato, S.; White, J. M. *J. Phys. Chem.* **1981**, *85*, 592.
(45) Kawai, T.; Sakata, T. *J. Chem. Soc., Chem. Commun.* **1980**, 694.
(46) Pichat, P.; Herrmann, J. M.; Disdier, J.; Courbon, H.; Mozzanega, M. N. *J. Chim.* **1981**, *5*, 627.
(47) Izumi, I.; Fan, F. R.; Bard, A. J. *J. Phys. Chem.* **1981**, *85*, 218.
(48) St. John, M. R.; Furgala, A. J.; Sammells, A. F. *J. Phys. Chem.* **1983**, *87*, 801.
(49) Izumi, I.; Dunn, W. W.; Wilbourn, K. O.; Fan, F. R.; Bard, A. J. *J. Phys. Chem.* **1980**, *84*, 3207.
(50) Pichat, P.; Mozzanega, M.-N.; Disdier, J.; Herrmann, J.-M. *Nouv. J. Chim.* **1982**, *11*, 559.
(51) Domem, K.; Kudo, A.; Onishi, T. *J. Phys. Chem.* **1986**, *90*, 292.
(52) Domem, K.; Kudo, A.; Onishi, T. *J. Catal.* **1986**, *102*, 92.
(53) Duonghong, D.; Borgarello, E.; Gratzel, M. *J. Am. Chem. Soc.* **1981**, *103*, 4685.

Therefore, the composite C−BIO loaded with nanosized Pt or NiO_x can be expected to exhibit high photocatalytic activities.

3.4. Band Structures of the Composite C−BIO. The band edge potential levels of Cr−$Ba_2In_2O_5$ and Cr−In_2O_3 play a crucial role in determining the flowchart of photoexcited charge carriers in C−BIO. Therefore, it is of importance to clarify the relative potential levels of individual band edges. For simplicity, we first consider the band structures of $Ba_2In_2O_5$ and In_2O_3. Using the CASTEP program package, the band structures of In_2O_3 and $Ba_2In_2O_5$ were calculated with the crystal lattice parameters and atomic coordinates and occupation factors[35,36] by the plane−wave−density function theory (DFT). The results showed that the valence band edges of both In_2O_3 and $Ba_2In_2O_5$ were determined by O 2p orbitals locating at the same potential level, whereas their conduction band edges were mainly formed by In 5s orbitals located at different potential levels (i.e., the In 5s orbitals in $Ba_2In_2O_5$ were higher than that in In_2O_3). In other words, the calculated band gap energy of In_2O_3 was smaller than that of $Ba_2In_2O_5$, being consistent with those estimated from the UV−vis reflectance spectra. These results indicated that the conduction band bottom of In_2O_3 was higher than that of $Ba_2In_2O_5$. Concerning the band structures of Cr−$Ba_2In_2O_5$ and Cr−In_2O_3, the behavior of Cr 3d orbitals within the forbidden gap of an oxide semiconductor should be considered first. As demonstrated in Cr−TiO_2[26−31] and Cr−$SrTiO_3$,[32] the occupied Cr 3d orbitals are usually located at a definite potential level (e.g., ∼2.2 eV for Cr-doped TiO_2[31]) below the conduction band bottom. It means that in a Cr-doped oxide, while the conduction band edge is not affected by Cr doping, the potential level of occupied Cr 3d orbitals is actually related to the potential level of conduction band bottom in the pure oxide (i.e., the higher the conduction band bottom, the higher the occupied Cr 3d orbitals are located). This can be understood easily because the doped Cr^{3+} generally substitutes for the cations that construct the conduction band of an oxide. As shown in Figure 2, since the band gap energy of Cr−In_2O_3 is smaller than that of Cr−$Ba_2In_2O_5$, we can conclude that the conduction band bottom of Cr−In_2O_3 is lower than that of Cr−$Ba_2In_2O_5$. From the UV−vis absorption spectra as shown in Figure 2, the difference of band gap energies between Cr−In_2O_3 and Cr−$Ba_2In_2O_5$ was estimated to be ∼0.12 eV, which was little bit smaller than that between In_2O_3 and $Ba_2In_2O_5$ (∼2.88 vs ∼3.02 eV). It indicated that the potential level of Cr 3d orbitals in Cr−$Ba_2In_2O_5$ was slightly higher than that in Cr−In_2O_3. In other words, the valence band top of Cr−$Ba_2In_2O_5$ was slightly higher than that of Cr−In_2O_3, although the Cr 3d orbitals might only form a shallow band close to O 2p. In fact, the experimental results also confirmed the aforementioned deductions. From Table 1, we noticed that Cr−$Ba_2In_2O_5$ showed a higher activity for H_2 evolution, whereas Cr−In_2O_3 showed a higher activity for O_2 evolution. Since the photocatalytic activity usually depends on the respective overpotential needed for evolution of either H_2 or O_2, it is reasonable to deduce that the band edges of Cr−$Ba_2In_2O_5$ lie at more negative positions than those of Cr−In_2O_3. Similar results have also been observed in Cr−TiO_2 and Cr−$SrTiO_3$ (i.e., Cr−$SrTiO_3$ showed a higher H_2 evolution rate than Cr−TiO_2 since the conduction band level of $SrTiO_3$ is slightly more negative than that of TiO_2).[32] For the previous considerations, the overall band structures, charge excitation, separation and transportation charts, and redox reactions in the C−BIO system are schematically illustrated in Figure 7. As an ohmic contact was assumed to bridge between the Cr−$Ba_2In_2O_5$ and Cr−In_2O_3 in the composite C−BIO system, the photoexcited electrons in the conduction band of Cr−$Ba_2In_2O_5$ were quite easy to fall down to the conduction band of Cr−In_2O_3, while the photoexcited holes in the valence band of Cr−In_2O_3 were likely to jump up to the valence band of Cr−$Ba_2In_2O_5$. The redox reactions were able to take place on the surface of Cr−In_2O_3 to evolve H_2 and on the surface of Cr−$Ba_2In_2O_5$ to evolve O_2, respectively. In this way, both H_2 and O_2 could be evolved simultaneously by splitting water in the C−BIO system. It is worthy to point out that, in addition to the conduction band edge offset, the valence band edge offset in C−BIO formed by the doped Cr 3d orbitals can be regarded as the most crucial reason accounting for the enhanced activities of C−BIO in comparison with those of BIO ($Ba_2In_2O_5$/In_2O_3), in which no valence band edge offset but conduction band edge offset exists between $Ba_2In_2O_5$ and In_2O_3. It maybe argued that the Schottky barrier should occur at the interface of Cr−$Ba_2In_2O_5$/Cr−In_2O_3, provided that both Cr−$Ba_2In_2O_5$ and Cr−In_2O_3 are *n*-type semiconductors. We think that the space charge region between the nanoscaled Cr−$Ba_2In_2O_5$ and Cr−In_2O_3 particles is too small to form the Schottky barrier, thus allowing for quantum mechanical tunneling of the photoinduced charge carriers.[54] Even if the Schottky barrier might be formed at the interface of Cr−$Ba_2In_2O_5$/Cr−In_2O_3 with larger sizes, the barrier height could be effectively lowered by the alloy created at the interface of Cr−$Ba_2In_2O_5$/Cr−In_2O_3 as mentioned in section 3.1. Therefore, this Schottky barrier can be overcome easily by the potential offsets between the band edges of Cr−$Ba_2In_2O_5$ and Cr−In_2O_3. Moreover, this Schottky barrier, as in the case

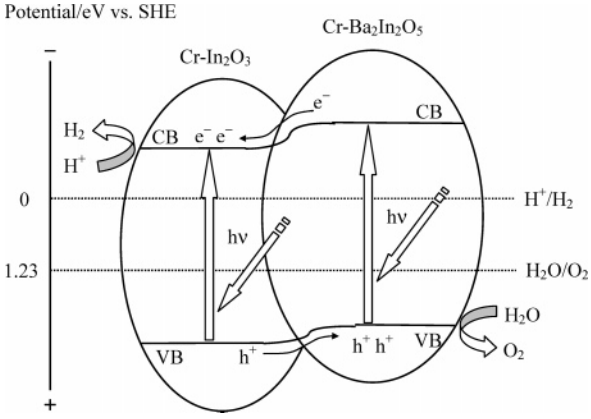

Figure 7. Scheme of the overall band structures, charge excitation, separation, and transportation charts and redox reactions for H_2 and O_2 evolution in the C−BIO system. The potential offset between the valence band edges could be ascribed to the different potential levels of Cr 3d orbitals in Cr−In_2O_3 and Cr−$Ba_2In_2O_5$, respectively. See text for details.

(54) Hummel, R. E. *Electronic Properties of Materials*; Springer-Verlag: Berlin, 1993.

of the metal/semiconductor interface, could also improve the charge carrier separation ability of C−BIO.[2]

For a single-phased oxide semiconductor under light irradiation, electrons are excited from valence band to conduction band, resulting in the formation of electron/hole pairs over the band gap. By the redox reactions at the conduction band and valence band, H_2 and O_2 are produced, respectively. Unfortunately, the rapid recombination of the photoexcited electron/hole pairs is likely to occur, which is thought to be an important reason for the difficulty of O_2 formation in a conventional photocatalysis system using a single-phased oxide semiconductor.[2] For a composite semiconductor system with different components being contacted ohmically, the intraparticle charge excitation and interparticle charge separation and transportation can proceed as multiple heterojunctions conceptually.[34] If the band edges of individual semiconductors are suitable for H_2 and O_2 evolutions, respectively, redox reactions in the well-contacted composite semiconductor system can behave, in principle, like a single-phased semiconductor. The difference is that, in comparison with a single-phased semiconductor, the charge excitation and separation for a composite semiconductor system proceed in a more complicated zigzag manner. The advantage is the improvement of photoexcited charge separation ability in a composite semiconductor system,[55,56] in which the band edge offset between the individual semiconductors provides the potential for the transportation of photoexcited charges along a preferable route, rendering the separation of photoexcited electrons and holes.

In terms of the importance of potential offsets between the band edges of individual materials in a composite oxide semiconductor system, it is necessary to recognize that the formation of a valence band offset is usually more difficult than the formation of conduction band offset between two oxide semiconductors with different band gap energies providing that the valence band edges of oxide semiconductors determined by O 2p orbitals are nearly at the same potential level. As discussed previously, the present C−BIO system showed us that the Cr 3d orbitals played a very important role in forming the potential offset between the valence band edges of $Cr-Ba_2In_2O_5$ and $Cr-In_2O_3$. To some extent, doping of foreign elements to create a new valence band above O 2p is indispensable to the formation of valence band offset between individual constituents in a composite oxide semiconductor system. In general, a composite semiconductor system applicable for photocatalytic water splitting with improved efficiency should be satisfied with the following conditions: the band edges of individual semiconductors are suitable for the redox reactions of H_2 and O_2 evolution; band edge offsets exist between the coupled semiconductors. It is expected that the interfacial charge-transfer kinetics and, thus, the total light harvesting efficiency of photocatalytic reaction can be promoted in a nanostructured composite semiconductor system.

4. Conclusions

A novel composite photocatalyst system—Cr-doped $Ba_2In_2O_5/In_2O_3$ (C−BIO) oxide semiconductors—synthesized simply by solid-state reactions has been found to show enhanced activities for water splitting under both UV and visible light irradiations. In comparison with the individual components with or without Cr doping, the composite C−BIO system with compatible band edges suitable for H_2 and O_2 evolution was advantageous in photoinduced charge carrier separation and migration due to the existence of potential offsets between the band edges of individual materials $Cr-Ba_2In_2O_5$ and $Cr-In_2O_3$ in C−BIO, which were assumed to be bridged properly by an ohmic contact, thus rendering the promoted photocatalytic activities. The present study suggests that designing a nanocomposite semiconductor system with tailored properties has been proven to be a promising alternative approach for the development of high efficient photocatalysts for overall water splitting.

Acknowledgment. The authors thank Drs. Junwang Tang and Tetsuya Kako for valuable discussions.

Supporting Information Available: Additional HRTEM images of C−BIO powder samples and theoretically calculated band structures and total density of states (DOS) of In_2O_3 and $Ba_2In_2O_5$. This material is available free of charge via the Internet at http://pubs.acs.org.

CM0477117

(55) Nasr, C.; Hotchandani, S.; Kamat, P. V. *J. Phys. Chem. B* **1998**, *102*, 10047.
(56) Vinodgopal, K.; Bedja, I.; Kamat, P. V. *Chem. Mater.* **1996**, *8*, 2180.